Technical Report 1403
April 1991

Fiber-Optic Refractionsonde

K. D. Anderson
C. M. Young

NAVAL OCEAN SYSTEMS CENTER
San Diego, California 92152–5000

J. D. FONTANA, CAPT, USN
Commander

H. R. TALKINGTON, Acting
Technical Director

ADMINISTRATIVE INFORMATION

This work was conducted under project RU35G80 of the Block Program. Block NO1A is managed by Naval Ocean Systems Center under the guidance and direction of the Office of Naval Technology. The work was funded under program element 0602435N and was performed by members of Code 543 and 946, Naval Ocean Systems Center, San Diego, CA 92152-5000.

Released by
R. A. Paulus, Head
Tropospheric Branch

Under authority of
J. H. Richter, Head
Ocean and Atmospheric
Sciences Division

MA

SUMMARY

OBJECTIVE

To demonstrate the feasibility of using a fiber-optic link to a modified radiosonde to determine refractive profiles for the Integrated Refractive Effects Prediction System and the Tactical Environmental Support System tactical decision aids under emission control (EMCON).

RESULTS

1. The 250-μm buffered optical fiber was found strong enough to handle the stresses involved with balloon takeoff and flight using the spinning-reel wind deployment technique.

2. Receiving, filtering, and amplifying the signals proved adequate for the ground station.

CONCLUSIONS

The refractionsonde, as a whole, functioned as expected and reliably transmitted the meteorological data to the ground station. A simple, nonradiating data link from the refractionsonde instrument package to the ground station receiver is feasible.

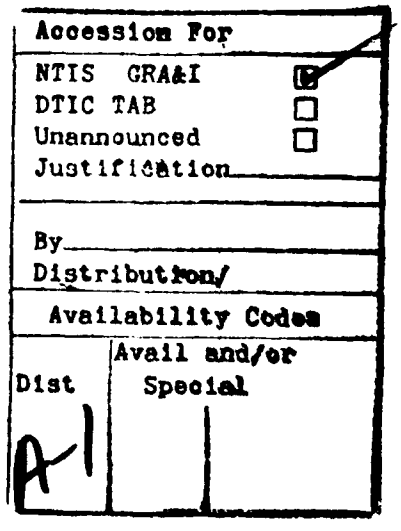

CONTENTS

FIGURES

CONTENTS (continued)

TABLES

INTRODUCTION

Vertical distribution of refractivity in the lower atmosphere can strongly affect the performance of shipboard radar, communication, and weapon systems (Hitney et al., 1985). The most dramatic refractive effects are those caused by surface-based ducts. Propagation assessment systems, such as the Integrated Refractive Effects Prediction System (IREPS) and the Tactical Environmental Support System (TESS), are used by operational forces to generate tactical decision aids (TDAs) tailored to assist in evaluating radar, communication, and weapon system performance (Patterson et al., 1987; Patterson, 1988). IREPS and TESS require as inputs measurements of the vertical distribution of refractivity to create the TDAs.

Current techniques for measuring the distribution of refractivity in the atmosphere use airborne electronic refractometer sets (ERS), or balloon-borne meteorological packages called radiosondes. Both techniques are widely used. The ERS, installed aboard E-2C aircraft, is limited to carrier battle groups. Atmospheric measurements by the E-2C are secondary to its normal mission. A radiosonde radiates approximately 1 W of power at 403 MHz as it rises through the atmosphere, and therefore, not used during emission control (EMCON). In addition, data from the radiosonde are used for synoptic forecasting, which requires that the balloon achieve an altitude of 30,000 feet (400 mbar) for a "legal" sounding.

A ship operating in EMCON without ERS support has no means to sense or measure atmospheric conditions crucial to IREPS and TESS TDAs. Therefore, a program was started to achieve the following four purposes:

1. To sense, in a manner compatible with EMCON, the vertical refractivity distribution in the lower atmosphere required by IREPS and TESS
2. To detect all instances of surface-based ducting
3. To develop a prototype-expendable meteorological sensing package
4. To maintain full compatibility with existing radiosonde ground station receivers

BACKGROUND

Many radio frequency (RF) transmission schemes can be adapted to operate in EMCON: spread spectrum, burst mode, very low power transmission, and frequency agile, to name a few. These schemes assume that the threat receiver characteristics are known and can be defeated by one or more of these methods. One method to guarantee that transmissions are not intercepted is to transmit the data through a fiber-optic cable (FOC). The optical fiber approach requires the balloon to lift not only the instrument package but also the additional weight of the FOC. Field tests using fishing line to simulate an FOC were conducted in October 1985. These tests demonstrated that a standard meteorological balloon could lift both the instrument package and an FOC to reasonable altitudes.

Surface-based ducts thicker than 1000 m are rarely observed in the atmosphere. Since these ducts are responsible for the most severe propagation distortions on shipboard systems, the vertical extent of the atmospheric measurements can be limited to altitudes of less than 2000 m. Such a height restriction means that a sounding would not be usable for synoptic forecasts. The proposed meteorological sensor package is called a *refractionsonde* to emphasize the distinction between a legal sounding for synoptic forecasting and a sounding launched during EMCON to determine the refractive profile for IREPS and TESS TDAs.

Existing radiosonde sensors are adequate to determine the refractive profile. A commercially available radiosonde package from Vaisala, model RS-80, was selected as the prototype hardware baseline. This instrument contains temperature, humidity, and pressure sensors that are factory calibrated. The calibration coefficients are recorded onto a punched tape. Temperature, humidity, and pressure sensor readings are converted to voltage and multiplexed to a voltage-controlled oscillator (VCO) that encodes the data to a frequency between 5 and 10 kHz. A 403-MHz RF transmitter is modulated by the audio signal. On the ground, the RF is received by an ultrahigh frequency (UHF) receiver where the 403-MHz carrier is removed and the audio signal is output as a frequency-modulated square wave. The output is processed by a Vaisala PP11 unit that decodes the audio signal into raw data. Prior to balloon launch. the calibration coefficients are read into the PP11 from the punched tape. The coefficients are used to convert the raw data into real units. During the balloon's ascent, temperature, humidity, and pressure are displayed by the PP11 and converted to a serial (RS-232) bit stream for output to a computer.

Converting the RS-80 radiosonde to a prototype refractionsonde is a straightforward engineering effort. The RF transmitter is replaced with a light-emitting diode (LED). An FOC is connected to the LED, and the other end of the FOC is connected to a photosensitive detector. The encoded audio signal is injected into the FOC and converted back to a voltage by the detector. The detector signal is filtered to recover the audio-frequency square wave, amplified, and output directly to the PP11 processor, bypassing the need for a UHF receiver. In addition, the original package of the RS-80 radiosonde is preserved.

TRANSMITTER AND RECEIVER

The RS-80 radiosonde consists of a circuit board containing a UHF transmitter, a sensor/encoder box, a 19-volt water-activated battery, and a transmitting antenna, all housed in a small foam package. The fiber-optic transmitter is designed to fit in the RS-80 foam package, and to use the existing radiosonde sensors and encoder. The radio transmitter is removed from the circuit and replaced with an optical LED transmitter. The 19-volt water-activated battery that powers the RS-80 sensor and encoder circuits is replaced with two lightweight, air-activated 8.4-volt batteries in series. A lightweight, 3-volt, lithium battery drives the optical transmitter. Weight and size of the components are major considerations. The circuit board and components were designed to be as small and light as possible. The RS-80 transmitter, fully equipped but without the water-activated battery, weighs 61.5 g. The optical transmitter package, without the air-activated batteries, weighs 82.2 g.

The signal from the encoder is a square wave with four different frequencies representing the synchronization signal, temperature, pressure, and humidity data. The modified transmitter does not change the format of this signal, but converts it to an optical signal. Therefore, the signal requires only detection, amplification, and filtering to make it suitable for the PP11 processor. The ground receiver has no size or weight restrictions, but must be portable and capable of remote hookup to the FOC endpoint. The output of the receiver is a 5-volt square wave to match the input requirements of the PP11.

Figure 1 is the transmitting and receiving circuit. The signal from the radiosonde VCO, containing the meteorological data, is shifted to the correct voltage range by a clamper and fed through a switching transistor to the LED for transmission through the FOC. A silicon detector picks up the signal and sends a proportional current to a transimpedance preamp. The detected signal is filtered by an active, three-pole, low-pass Bessel filter with a corner frequency at 11 kHz to reject the high-frequency noise and by a blocking capacitor to filter the low-frequency noise. Automatic gain control (AGC) is provided by the multiplier, peak detector, and adder circuits. The resulting waveform is squared up through a comparator and output to the PP11 processor. Figures 2 and 3 are the schematic diagrams of the refractionsonde transmitter and receiver.

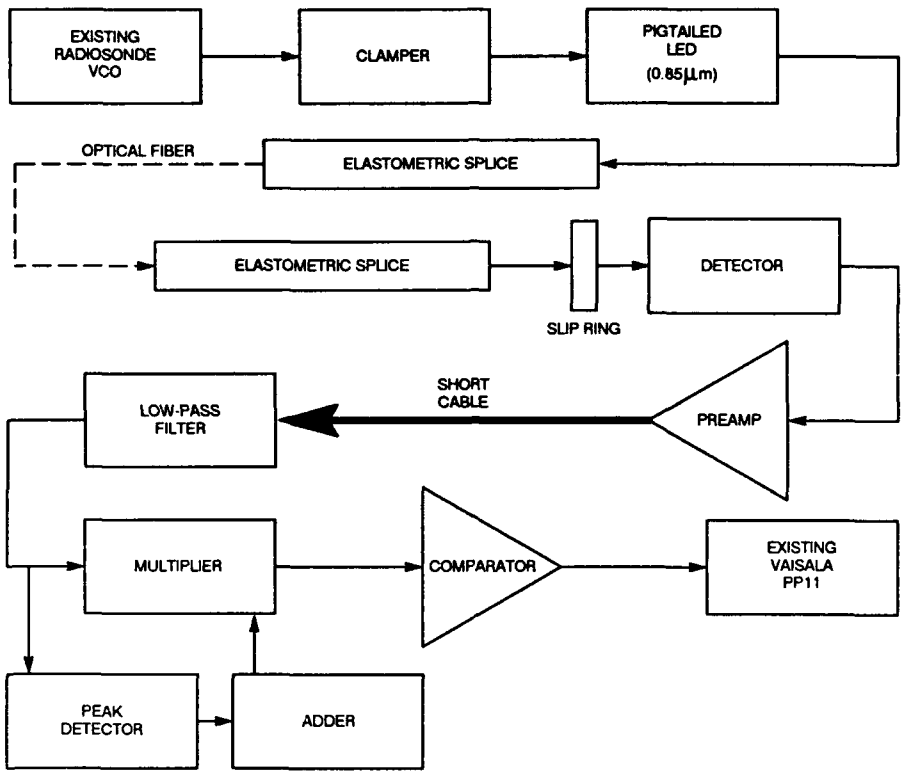

Figure 1. The refractionsonde transmitter and receiver circuits.

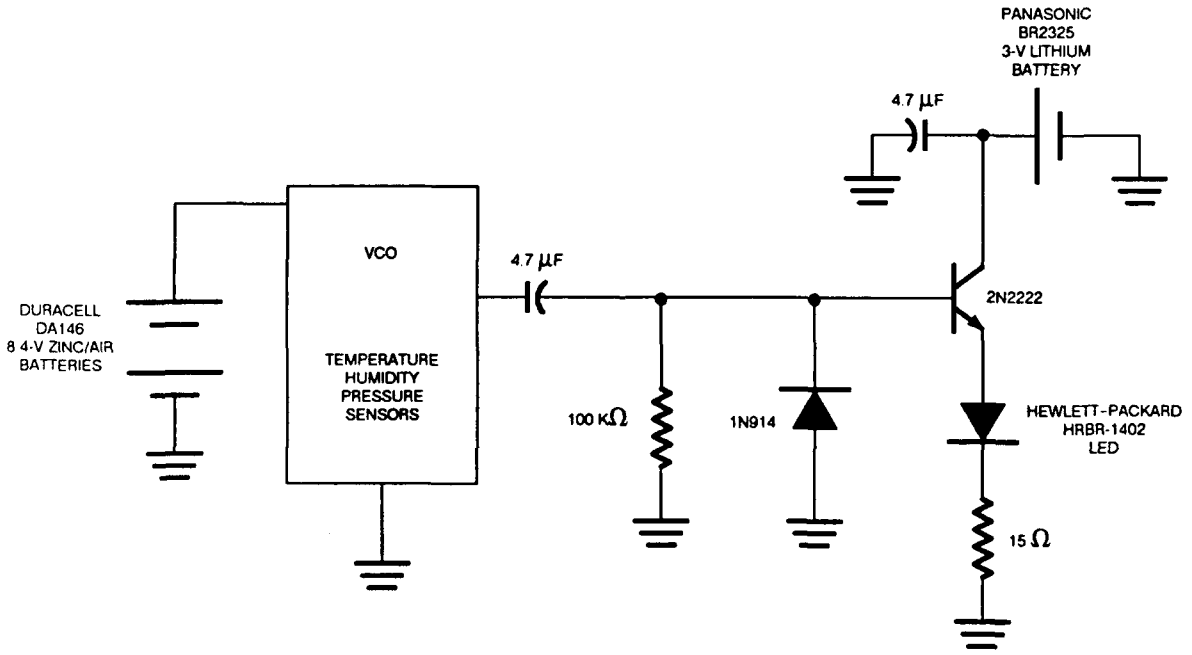

Figure 2. Refractionsonde transmitter schematic.

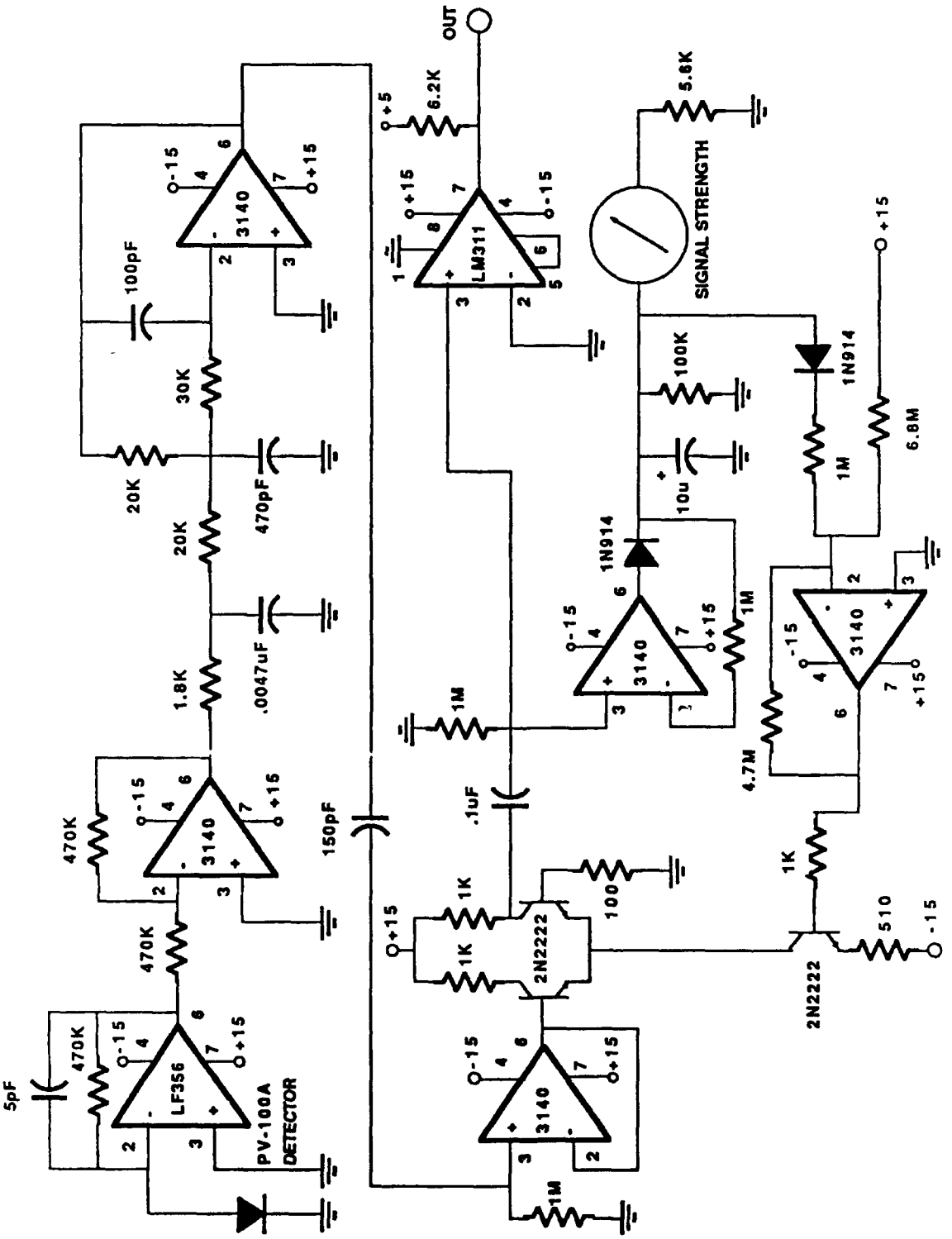

Figure 3. Refractionsonde receiver schematic.

FIBER-OPTIC CABLE DEPLOYMENT SYSTEM

The design objectives of the FOC deployment system are to develop an inexpensive system that can smoothly payout a buffered FOC as the balloon rises through the lower atmosphere Two deployment techniques were investigated. An active reel technique was used to evaluate the dynamics of cable payout. Passive techniques, using two different winds of cable, were examined to assess simplicity of construction and reliability of payout with minimal loss through the FOC.

TETHER REEL

Preliminary tests were conducted on 3 March 1987 to determine the suitability of an FOC tether by attaching a test balloon to a length of 1-kg test fishing leader deployed from a fishing reel. The drag on the reel could be increased to temporarily stop ascent of the balloon. There are two advantages to an adjustable drag reel system. First, the FOC can be deployed directly from the manufacturer's shipping reel without the need to rewind. Second, payout tension can be controlled to evaluate FOC loads and system dynamics.

Figure 4 shows the tether-reel mechanism developed to deploy the FOC. It accepts the Corning Glass Works spool used for single-mode optical fibers. These spools are dimensionally uniform, lightweight, can hold up to 6 km of 500-μm buffered FOC, and have provisions for accessing the inside end. The spool is mounted on a rotating shaft, which carries a disk brake on one end and an optical slip ring on the other.

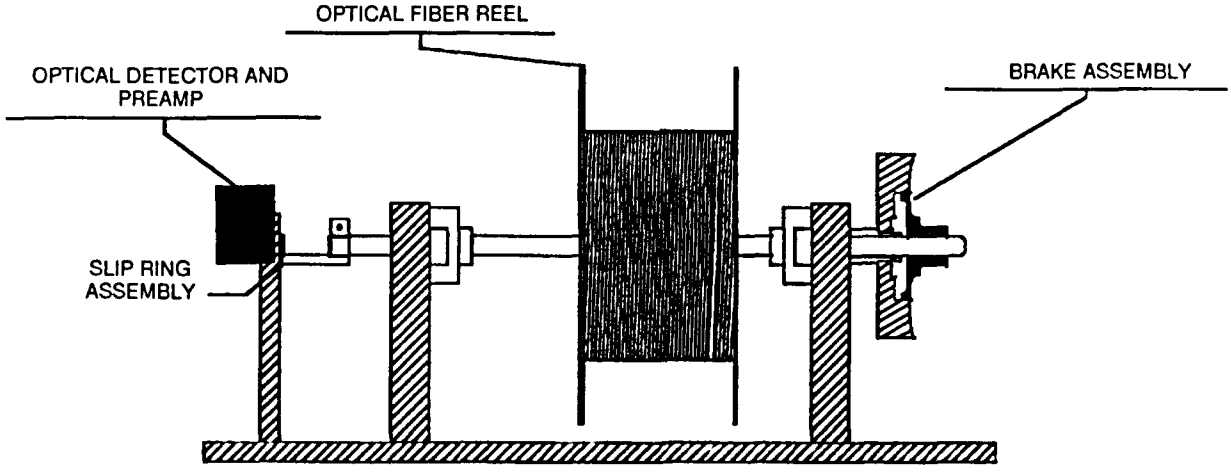

Figure 4. Tether-reel deployment mechanism.

The optical slip ring is an Amphenol 906 fiber-optic connector mounted on the axis of the shaft. A silicon photodetector with a 0.10-inch diameter active area is mounted on the frame adjacent to the rotating connector. A light baffle is used to exclude stray ambient light that could saturate the detector. The electronics are AC-coupled to further reduce interference. Signal variation over 360° of axis rotation was less than 5 percent.

Several undesirable characteristics of the tether-reel system were observed during flight testing. At the initial release of the balloon, the FOC experienced a shock load due to the inertia of the reel which needs to be rapidly accelerated. Although the FOC used during testing had sufficient elasticity to withstand the transient load (no failures were observed due to shock loading), it is clearly desirable to eliminate these shock loads. Smooth payout of the cable was observed with the brake set such that reel backlash was minimized. This brake setting varied for each flight because of minor differences in the assembled equipment, balloon lift, and wind speed. The alignment of the optical slip ring was observed to be critical. Small changes in the position of the ring caused strong fluctuations in signal strength and reliability of the transmitted data.

PASSIVE DEPLOYMENT

The goals of a passive deployment mechanism are to

1. reduce the transient load on the FOC imposed during launch,
2. eliminate the optical slip ring,
3. eliminate all controls and adjustments (brake), and
4. be of simple and inexpensive construction.

Two passive deployment systems were selected for testing. One employed a figure-eight wind of the FOC, which was packaged in a box with a deployment guide built into its top. The other was based upon a spinning-reel in a casting configuration. A drum was wound with the FOC that was deployed by pulling it over one end, which had a specially shaped flange to reduce the severity of the bend at that point.

Figure-Eight Wind

The figure-eight wind was intended to eliminate tangling of the FOC while allowing a near-zero tension deployment. Coil and hardware configuration are shown in figure 5. The launch tension transient is virtually eliminated with this system because only a short length of FOC must be accelerated as the balloon is launched. An optical slip ring is not required because the FOC deployment package does not rotate.

Automated equipment that can produce a figure-eight wind was unavailable so coils were wound by hand. These coils tended to shift within the box, causing crossovers in the FOC during transportation. A foam insert was used to hold the FOC snugly within the box to reduce the crossover problem.

A 2.5-km length of 250-μm buffered FOC was wound to test the packaging concept. The base attenuation of this fiber was 0.72 dB/km at 1300 nm. Optical attenuation of the packaged fiber was measured with an optical time-domain reflectometer (OTDR) and is shown in figure 6(a) and 6(b). Figure 6(a) shows the OTDR response of the FOC on the reel as it was shipped from the manufacturer. Figure 6(b) illustrates the OTDR response of the FOC wound as a figure-eight in the deployment package. The excess attenuation is 0.7 dB/km. The weight of the upper layers of the FOC pressing down on the crossover points in the coil cause additional bending losses. The total optical loss through the 2.5-km length of FOC was sufficiently low that the optical transmitter and receiver were able to operate. However, if the coil length were to be increased to 5 km or longer, a higher power LED transmitter or a more sensitive receiver would be required.

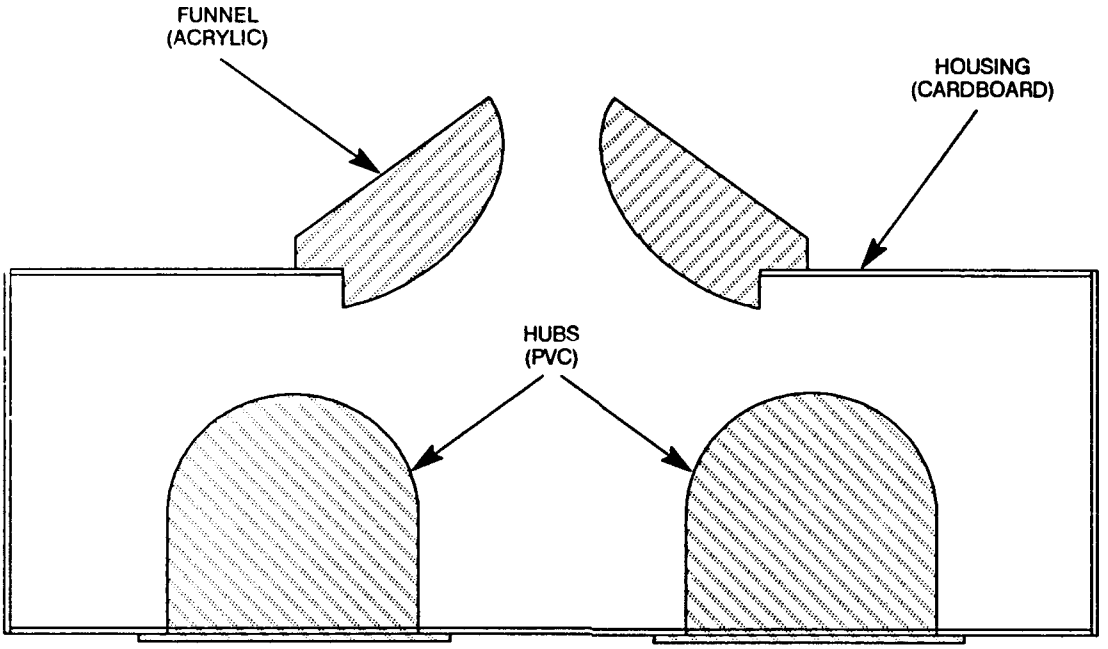

Figure 5. Passive figure-eight wind deployment mechanism.

(A)

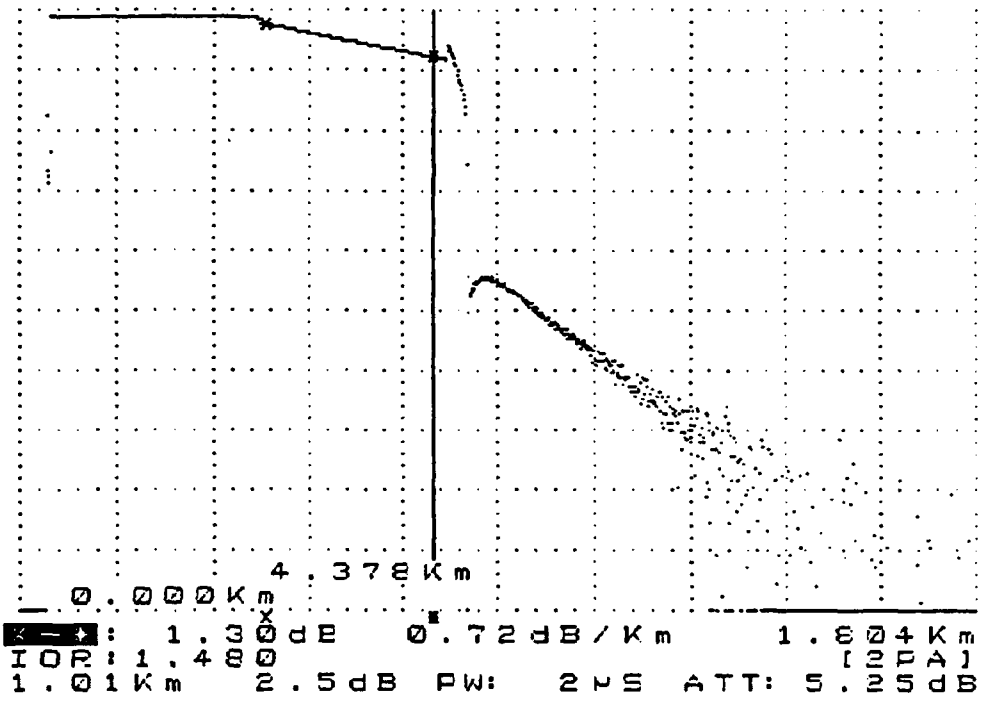

(B)

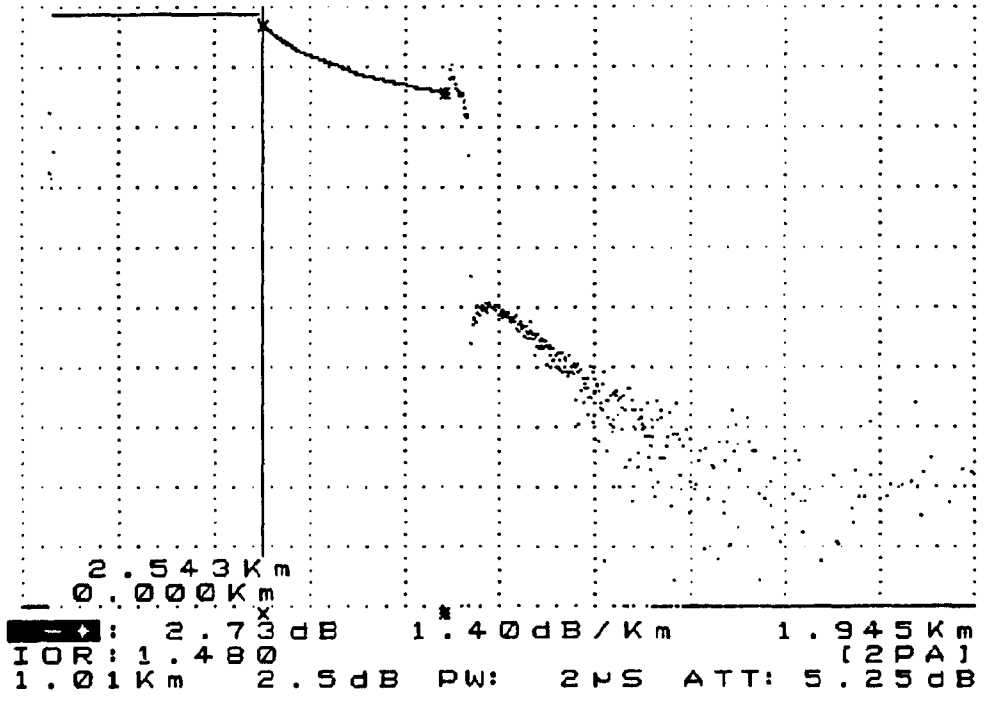

Figure 6. (a) OTDR response of the 250-μm buffered FOC as it was shipped from the manufacturer. (b) OTDR response of the FOC wound in the figure-eight deployment pack.

Flight tests revealed severe problems with the figure-eight wind concept. Initial launch of the refractionsonde was successful with minimal, snap, or shock loading. However, within several seconds of launch, the ascending balloon began to pull multiple loops of FOC from the box, resulting in tangles and a broken FOC after 15 seconds. The shifting of the FOC in the box either during winding, transportation, or deployment caused the pulling of multiple loops. Loops would be pulled from the box and the FOC would break in bending at very low tension. Because of problems with winding, package stability, excess optical attenuation, and deployment, the figure-eight technique was abandoned in favor of a spinning-reel technique.

Spinning-Reel Wind

The hardware for the spinning-reel system is shown in figure 7. It consists of a drum with a flat flange on the bottom and a curved flange at the top, a housing, and a deployment guide. The FOC was wound using a computer-controlled winding in a low-angle, scramble-wind pattern with approximately 50 grams of tension. No pretwist was used because of the low torsional stiffness of the FOC. The spinning-reel packaging configuration proved to be extremely stable. The FOC showed no tendency to shift as with the figure-eight wind configuration. Figure 8 is an OTDR trace of a spinning-reel deployment pack. The excess attenuation induced by this winding technique was 0.4 dB/km and was uniform throughout the 2- and 5-km packs that were wound. Optical attenuation of a 5-km deployment pack was measured over a temperature range of −20°C to 60°C. Excess attenuation at −20°C was 0.02 dB/km and at 60°C was 0.8 dB/km. These changes were reversible with the attenuation returning to a baseline value of 1.0 dB/km at room temperature.

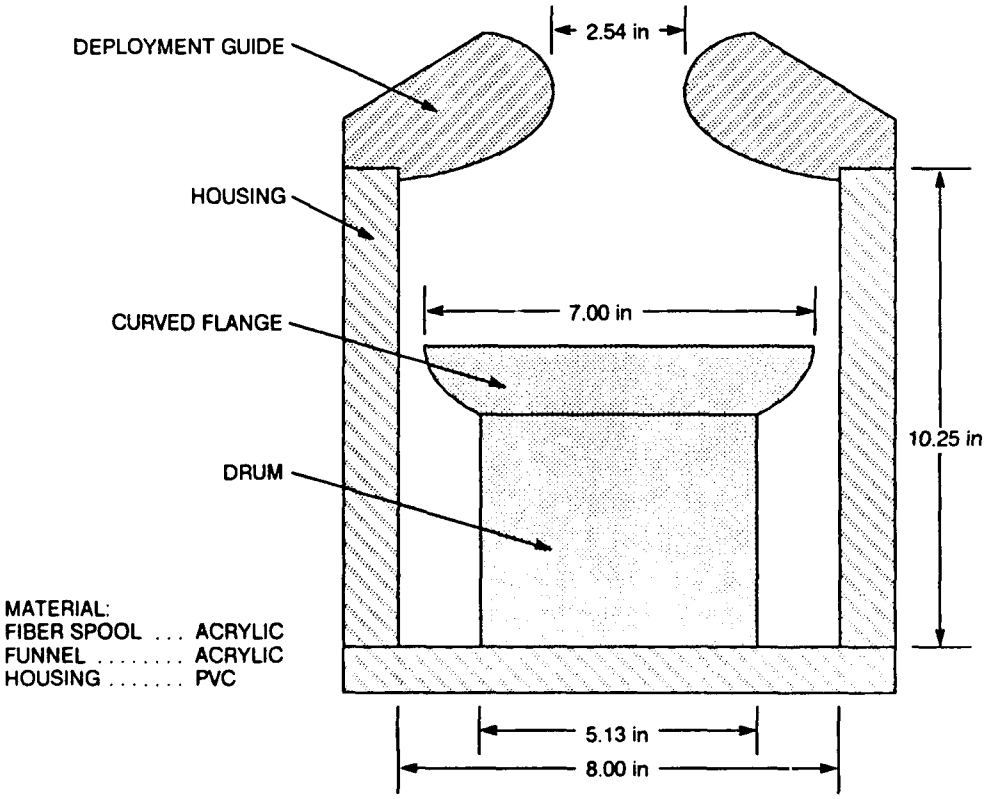

Figure 7. Passive spinning-reel wind deployment mechanism.

(A)

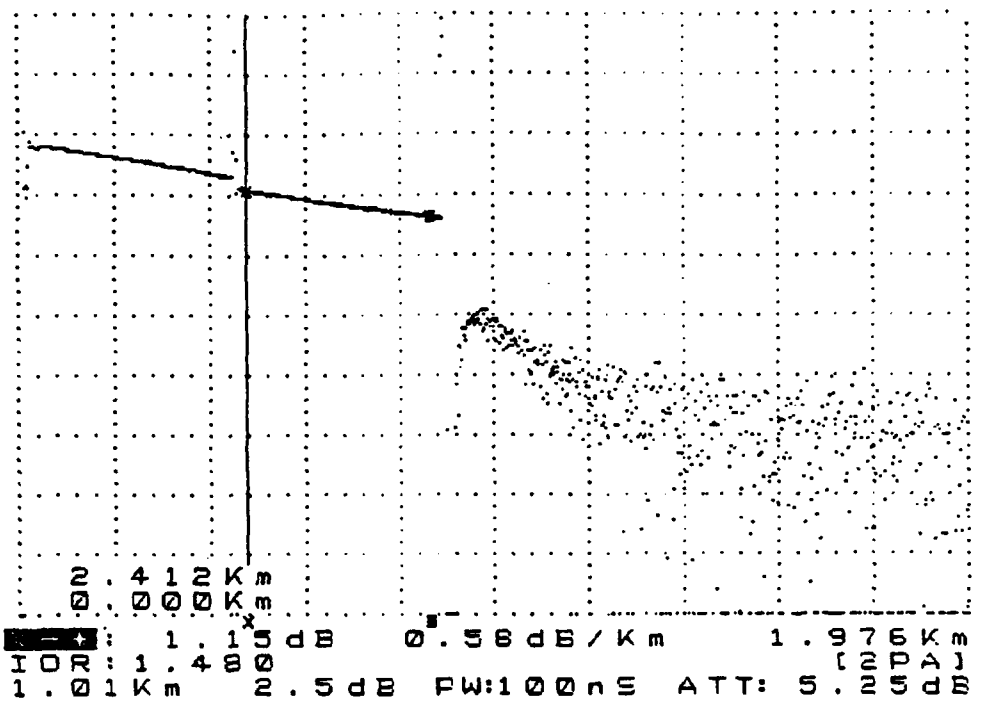

(B)

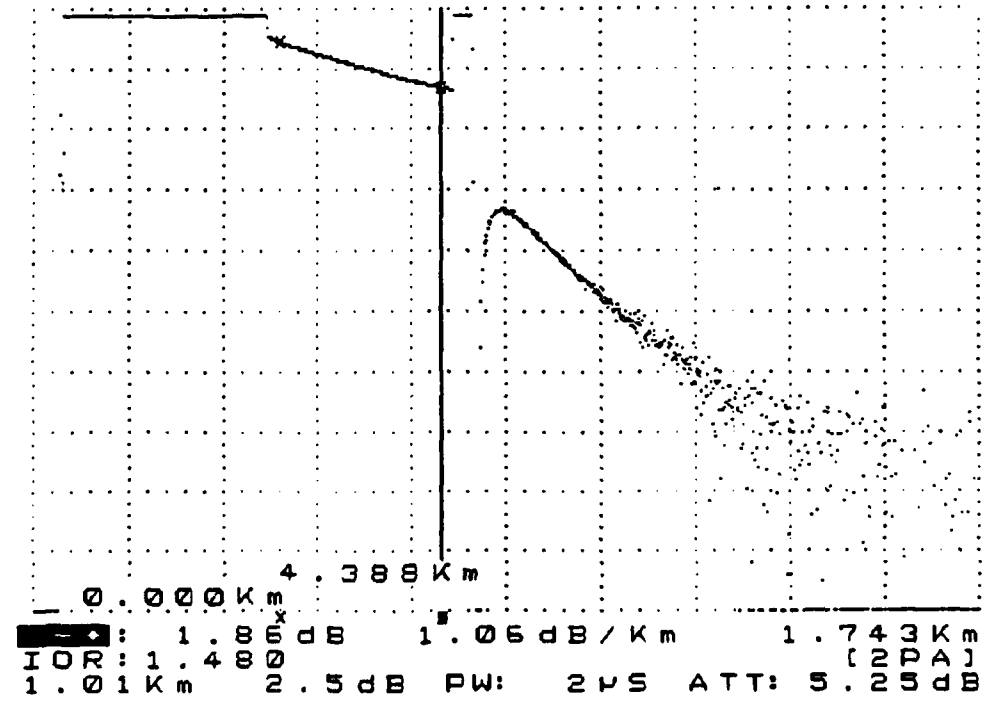

Figure 8. (a) OTDR trace of the FOC as it was shipped from the manufacturer. (b) OTDR response of the FOC wound in the spinning-reel deployment pack.

FIBER-OPTIC LINK

The fiber-optic link consists of a buffered, graded-index multimode optical fiber with no additional strengthening elements. A 100-kpsi proof test was specified for the fiber, which yields a minimum tensile strength of about 1 kg. The strength of such a fiber in short-gauge lengths tends to be much higher, near 5 kg. This characteristic turned out to be useful in allowing the FOC to withstand the minor shock loads it was subjected to at launch when the tether-reel mechanism was used. As the balloon rose and the FOC deployed, the elasticity of the fiber acted as a shock absorber and effectively reduced the transient loads in the tether. No significant signal degradation was observed.

Commercial telecommunications FOCs are available with buffer coatings of different diameters and materials. In the United States, the most common fiber buffer material is an ultraviolet (UV)-cured urethane acrylate with a diameter of either 250 or 500 μm. The 250-μm buffered cables are most commonly used for "loose tube" constructions, where the FOC is protected from microbending by encasing it in a small tube. The 500-μm buffers provide FOCs with greater microbending isolation and are most often used in direct stranding applications. A 500-μm buffered optical fiber was originally selected for the first tests of the refractionsonde link. The additional ruggedness and microbend isolation was believed to be desirable for use with a reel-type system. However, flight tests demonstrated that the wind drag on the 500-μm cable was not satisfactory for a reasonable deployment.

In a balloon tether deployment system, the weight and wind drag of the FOC are very important. The critical parameters for 250- and 500-μm buffered optical fibers are

a.	Fiber diameter	250 μm	500 μm
b.	Weight per 1000 m	70 g	260 g
c.	Drag coefficient (crossflow)	1.40	1.25

The drag coefficient of the 250-μm FOC is only slightly greater than the 500-μm cable. Also, the 250-μm cable will experience roughly one-half of the wind-drag force. The mass of the smaller fiber is one-fourth that of the larger one.

FLIGHT TESTS

26 JUNE 1987

The first flight test of the prototype fiber-optic refractionsonde was conducted on 26 June 1987 at Building 323, NOSC. The tether reel (figure 4) was used to deploy 2.2 km of 500-μm buffered FOC. At the time of the launch, wind speed was 4 to 5 m/s blowing from the northwest. Surface pressure was 1016.8 mbar at the launch height (33 m above mean sea level). A standard 100-g balloon was used to carry the refractionsonde package and the FOC.

Figure 9 shows the relative humidity and the air temperature recorded as the balloon ascended, plotted against pressure (mbar). The package rose to a pressure altitude of 860.7 mbar (1447 m) in an elapsed time of 11 minutes 11 seconds—nearly all of the FOC was deployed. At this altitude, the balloon burst and the package fell. Data were recorded during the descent to the ground and for an additional 51 seconds after impact. The descent trace is also shown in figure 9 (larger spacing between dots) and reasonably replicates the ascending profile. Table 1 lists the elapsed time (from launch), pressure,

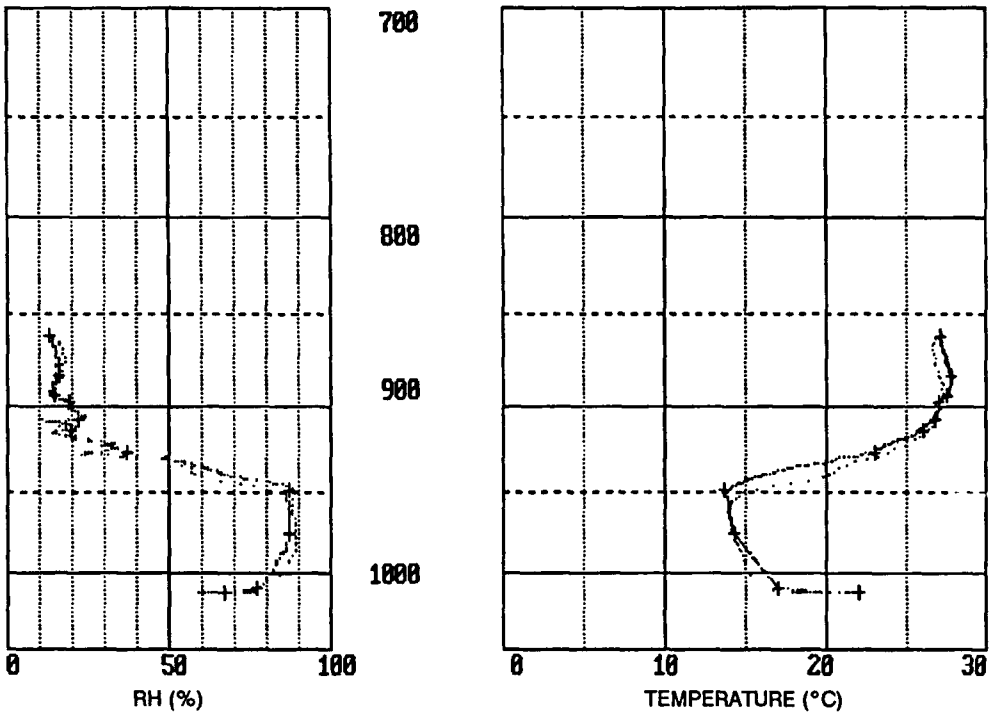

Figure 9. Pressure-altitude plot of temperature and relative humidity for the 1341 PDT, 26 June 1987 flight test.

Table 1. Data from 1341 PDT, 26 June 1987 flight test.

Time (s)	Press. (mbar)	Temp. (C)	RH (%)	Height (m)	M	dT (s)	dH/dT (m/s)	<dH/dT> (m/s)
0	1016.8	22.0	67	33.0	348.5			
44	1013.9	17.0	77	57.1	346.3	44	0.55	0.55
91	979.1	14.3	87	354.5	384.0	47	6.33	3.53
142	952.1	13.7	87	591.0	412.2	51	4.64	3.93
228	929.7	23.0	37	794.9	412.7	86	2.37	3.34
287	916.8	26.0	20	917.2	409.2	59	2.07	3.08
322	910.4	26.8	22	978.8	421.4	35	1.76	2.94
377	900.3	27.0	19	1077.4	430.0	55	1.79	2.77
410	896.5	27.5	15	1114.4	428.3	33	1.12	2.64
486	885.3	27.8	16	1225.5	445.3	76	1.46	2.45
671	863.3	27.1	13	1447.6	469.7	185	1.20	2.11

air temperature, relative humidity, height, modified refractivity (M units), time separation between levels (dT), ascent rate between levels (dH/dT), and average ascent rate (<dH/dT>).

As the balloon rose, the FOC began dragging on the ground. At the maximum altitude, the FOC was being pulled horizontally from the tether-reel mechanism. Approximately 150 m of FOC were estimated to be on the ground at the conclusion of the ascent. The probable cause of the FOC dragging on the ground appears to be excess wind drag on the cable.

Difficulties in controlling the tether-reel brake mechanism, alignment of the optical slip ring, and the excess wind drag on the 500-μm FOC led to the development of the passive deployment systems using the smaller diameter buffered cable.

5 JULY 1988

Two flights were conducted to test the spinning-reel and the figure-eight wind passive deployment mechanisms. Wind was 4 to 5 m/s blowing from the west. Figures 10 and 11 are plots of the temperature and humidity as the balloons rose; tables 2 and 3 list the data.

The first flight test of the day (at 1440 PDT, figure 10) was made using a 100-g balloon to pull the FOC (250 μm) from a spinning-reel wind pack. The package rose to an altitude of 486 m in 2 minutes 23 seconds. At this height, the balloon burst. The failure mode was assumed to be stress (both heat and mechanical) on the balloon, which may have been accentuated by filling the balloon approximately 15 minutes prior to launch.

The second flight of the day (at 1507 PDT, figure 11) was made using a 300-g balloon to pull the FOC from a figure-eight wind pack. The payout was poor as the refractionsonde immediately began pulling multiple loops of FOC. The failure mode was the FOC separation caused by knotting of the cable during payout. The figure-eight wind deployment scheme was abandoned after this test.

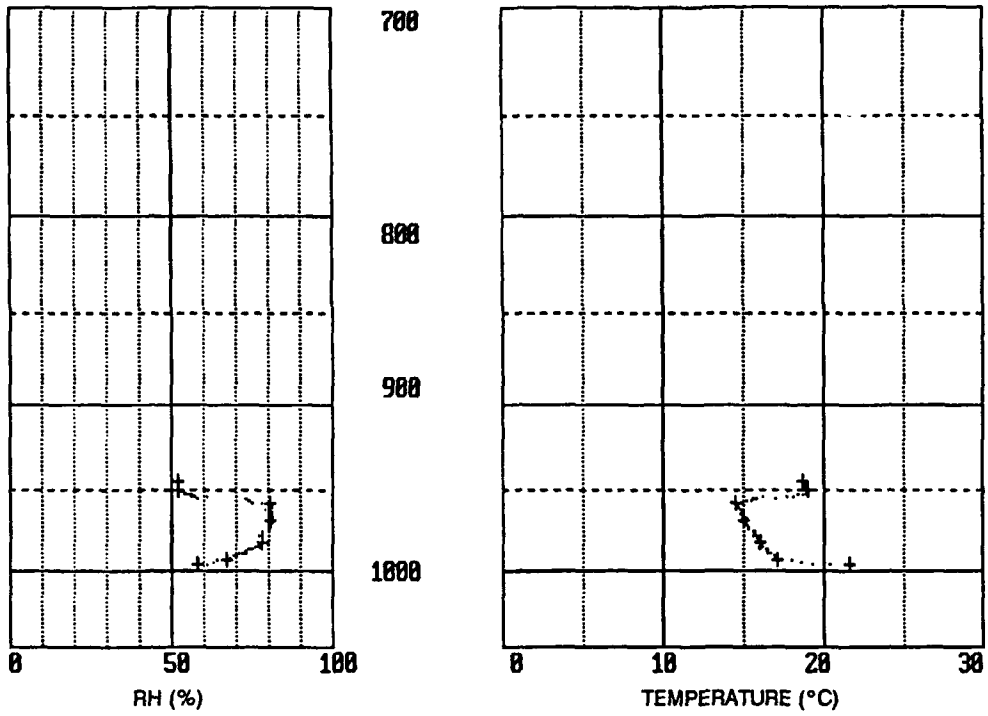

Figure 10. Pressure-altitude plot of temperature and relative humidity for the 1440 PDT, 5 July 1988 flight test.

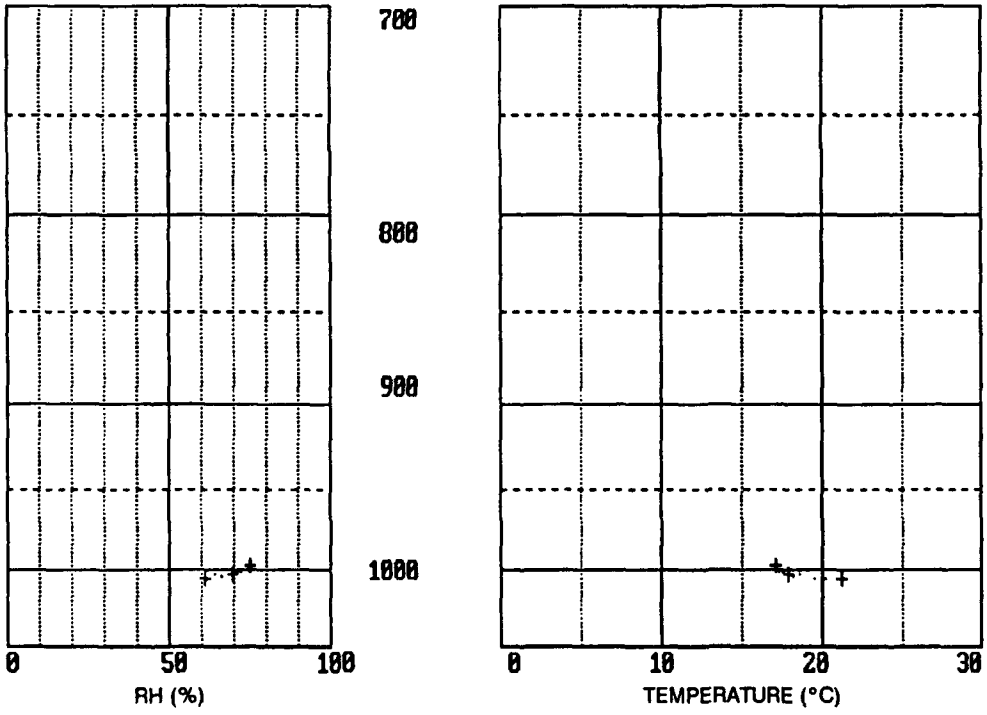

Figure 11. Pressure-altitude plot of temperature and relative humidity for the 1507 PDT, 5 July 1988 flight test.

Table 2. Data from 1440 PDT, 5 July 1988 flight test.

Time (s)	Press. (mbar)	Temp. (C)	RH (%)	Height (m)	M	dT (s)	dH/dT (m/s)	<dH/dT> (m/s)
0	999.9	21.6	58	33.0	332.8			
9	997.1	17.1	67	57.1	333.5	9	2.68	2.68
33	986.0	16.0	78	152.5	351.9	24	3.98	3.62
64	972.3	15.0	81	271.4	366.2	31	3.84	3.72
100	961.5	14.5	81	366.2	376.8	36	2.63	3.33
125	953.4	19.0	52	437.8	372.0	25	2.86	3.24
143	948.1	18.7	52	485.8	377.5	18	2.67	3.17

Table 3. Data from 1507 PDT, 5 July 1988 flight test.

Time (s)	Press. (mbar)	Temp. (C)	RH (%)	Height (m)	M	dT (s)	dH/dT (m/s)	<dH/dT> (m/s)
0	1009.7	21.2	61	33.0	337.6			
10	1006.9	17.9	70	57.1	340.3	10	2.41	2.41
22	1001.3	17.1	75	105.0	349.0	12	3.99	3.27

18 OCTOBER 1988

Three flights were made on this day to test the spinning-reel wind deployment pack. All three flights used 300-g balloons and 250-μm cable. Winds were calm to 2 m/s. Figures 12, 13, and 14 show the temperature and humidity profiles; tables 4, 5, and 6 list the data.

The first flight (0843 PDT, figure 12) used a 2.2-km length of FOC and rose to an altitude of 1354 m in 5 minutes 32 seconds. The full length of FOC was pulled out and the balloon was tethered for 20 seconds until the cable separated at the deployment pack. FOC separation was probably due to catching a small sharp edge of the pack.

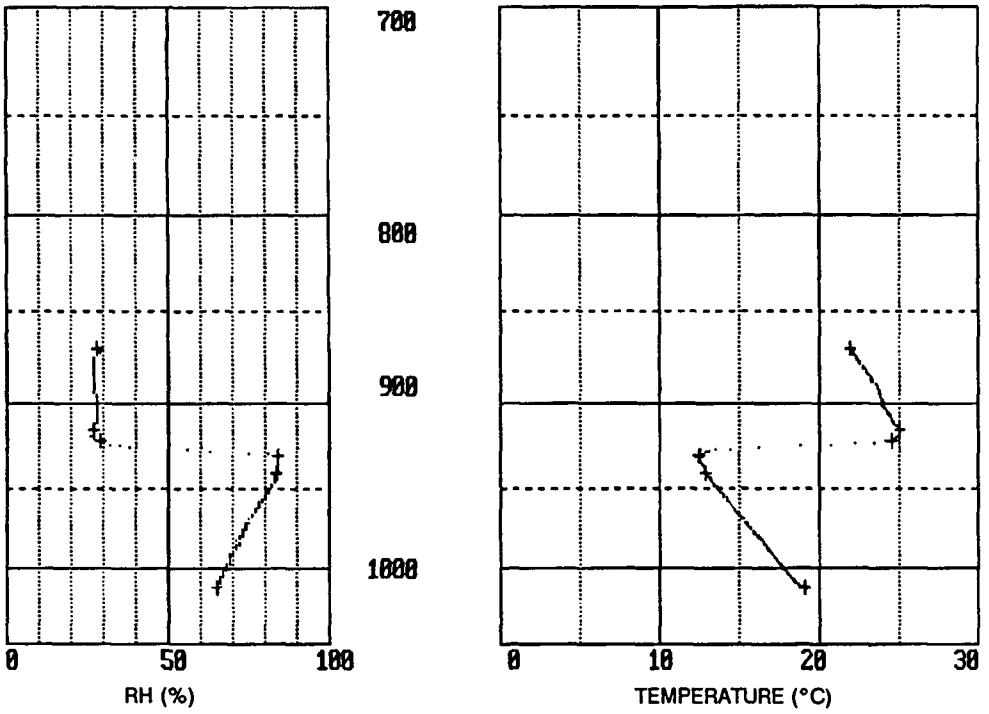

Figure 12. Pressure-altitude plot of temperature and relative humidity for the 0843 PDT, 18 October 1988 flight test.

Table 4. Data from 0843 PDT, 18 October 1988 flight test.

Time (s)	Press. (mbar)	Temp. (C)	RH (%)	Height (m)	M	dT (s)	dH/dT (m/s)	<dH/dT> (m/s)
0	1016.8	19.1	65	33.0	338.0			
164	944.2	12.9	84	663.9	417.0	164	3.85	3.85
185	933.6	12.5	84	758.0	428.3	21	4.48	3.92
208	924.6	24.5	29	842.0	410.8	23	3.65	3.89
221	918.1	25.0	27	903.2	416.7	13	4.71	3.94
332	871.8	21.9	28	1354.2	473.4	111	4.06	3.98

Table 5. Data from 0903 PDT, 18 October 1988 flight test.

Time (s)	Press. (mbar)	Temp. (C)	RH (%)	Height (m)	M	dT (s)	dH/dT (m/s)	<dH/dT> (m/s)
0	1018.2	19.0	57	33.0	330.5			
98	975.0	15.2	69	403.2	378.8	98	3.78	3.78

Table 6. Data from 0920 PDT, 18 October 1988 flight test.

Time (s)	Press. (mbar)	Temp. (C)	RH (%)	Height (m)	M	dT (s)	dH/dT (m/s)	<dH/dT> (m/s)
0	1018.2	19.3	57	33.0	331.1			
122	949.4	13.5	77	628.8	409.9	122	4.88	4.88
147	933.6	12.8	77	770.1	426.2	25	5.65	5.01
163	927.1	24.3	26	830.1	404.9	16	3.75	4.89
190	914.3	25.4	22	952.5	416.4	27	4.53	4.84
279	873.0	24.4	22	1356.5	469.0	89	4.54	4.74
411	831.4	18.3	31	1779.9	528.9	132	3.21	4.25
473	808.4	16.7	31	2018.6	559.0	62	3.85	4.20

The second flight (0903 PDT, figure 13) used a 5.5-km length of the FOC and rose to an altitude of 403 m. At this height, the string connecting the refractionsonde to the balloon separated at the refractionsonde, allowing the balloon to fly free. The refractionsonde package was recovered.

The third flight (0920 PDT, figure 14) used a 5.5-km length of FOC and rose to an altitude of 2018 m. Wind was fairly consistent at 2 m/s. Not all of the FOC was deployed, estimated 4.5 km, before signal was lost. It was assumed that the FOC separated some distance from the deployment pack, possibly at the splice on the refractionsonde.

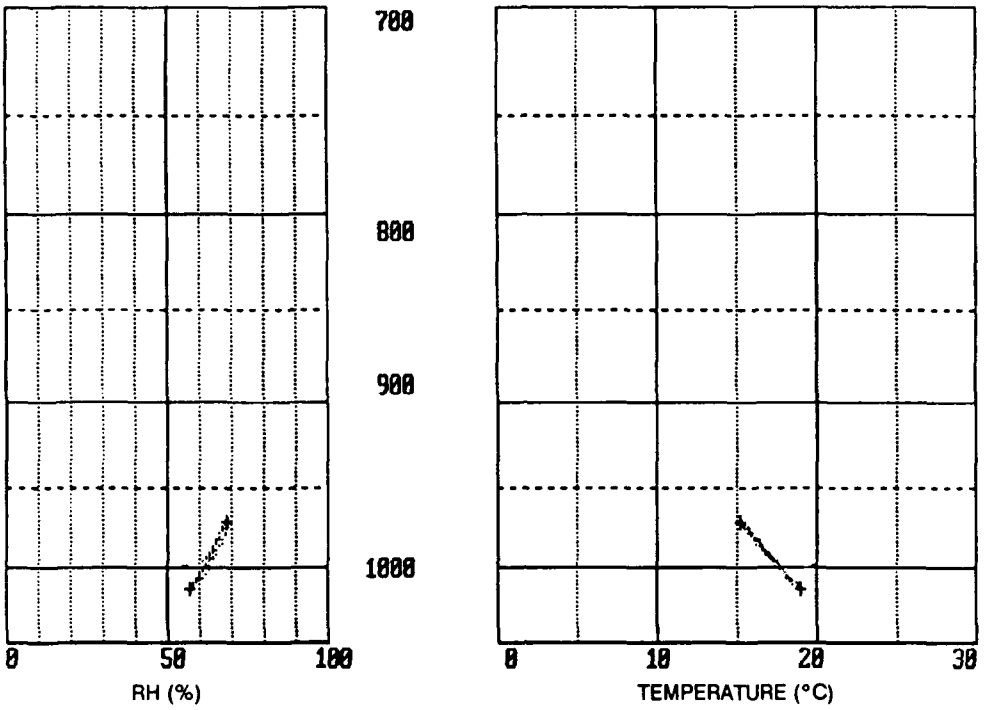

Figure 13. Pressure-altitude plot of temperature and relative humidity for the 0903 PDT, 18 October 1988 flight test.

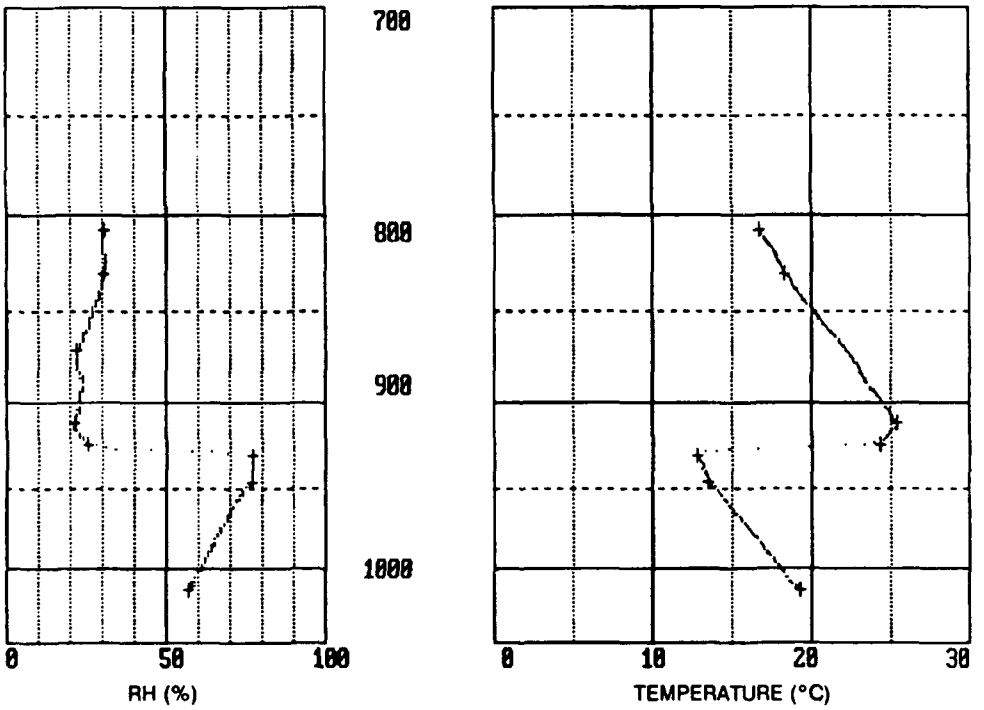

Figure 14. Pressure-altitude plot of tempe nd relative humidity for the 0920 PDT, 18 October 1988 flight test.

21 NOVEMBER 1988

One flight was made to test the spinning-reel wind pack. The temperature and humidity profiles are shown in figure 15 and the data are listed in table 7. The balloon was 300 g and the FOC was 2.2-km length of 250-μm cable. Winds were calm to 1 m/s.

The refractionsonde rose nearly straight up from the deployment pack and reached maximum altitude at 2191 m. All of the FOC was payed out.

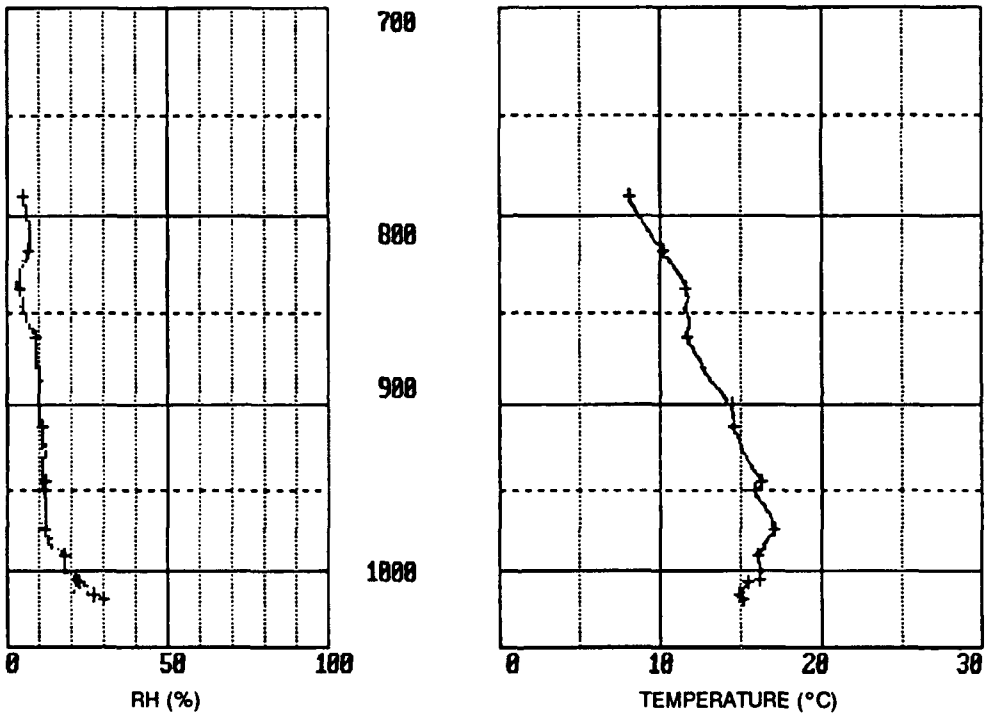

Figure 15. Pressure-altitude plot of temperature and relative humidity for the 0924 PST, 21 November 1988 flight test.

Table 7. Data from 0924 PST, 21 November 1988 flight test.

Time (s)	Press. (mbar)	Temp. (C)	RH (%)	Height (m)	M	dT (s)	dH/dT (m/s)	<dH/dT> (m/s)
0	1022.5	15.2	30	33.0	303.6			
7	1019.6	14.9	27	56.6	304.1	7	3.37	3.37
23	1011.1	15.5	23	127.6	309.6	16	4.44	4.11
27	1009.7	16.2	22	139.5	310.3	4	2.98	3.94
65	994.3	16.1	18	270.0	323.8	38	3.43	3.65
98	977.7	17.1	12	412.5	336.5	33	4.32	3.87
151	953.4	15.9	12	626.2	363.5	53	4.03	3.93
162	948.1	16.3	12	673.7	369.8	11	4.32	3.95
234	915.6	14.6	11	969.4	407.3	72	4.11	4.00
261	902.8	14.5	10	1087.3	421.6	27	4.37	4.04
363	864.5	11.7	9	1450.9	468.9	102	3.56	3.91
434	838.4	11.6	4	1707.6	499.0	71	3.62	3.86
488	818.7	10.2	7	1905.4	527.0	54	3.66	3.84
564	790.5	8.1	5	2194.6	565.1	76	3.81	3.83

31 JANUARY 1989

All of the previous testing was done from a land-based site. To assess the capabilities of the spinning-reel wind pack from a shipboard platform, the NOSC NMB-15 boat was used. This boat is 22 m in length, which allowed loading of the helium cylinders, receiver, and computer equipment on board. Four flights were made from this platform, stationed approximately 10 km offshore. All four flights used 250-μm FOC and 300-g balloons. Winds were calm to 2 m/s. Figures 16 through 19 show the measured temperature and relative humidity profiles. Tables 8 through 11 list the data.

The first flight (0953 PST, figure 16) used a 2.2-km length of FOC and rose to an altitude of 2216 m. The test was made with the boat under steerageway from the time of launch. The refractionsonde tethered and the FOC had to be physically cut to conclude the flight.

The second flight (1043 PST, figure 17) used a 5.3-km length of FOC and rose to an altitude of 3124 m. The package was launched with the boat under steerageway. After the initial ascent, the boat was sped up to approximately 3 m/s (6 knots). The FOC separated shortly after the full length was payed out.

The third flight (1110 PST, figure 18) used a 2.2-km length of FOC and rose to an altitude of 1573 m. Like the second flight, the refractionsonde was launched with the boat under steerageway, but shortly after launch, the boat was sped up to 6 m/s (12 knots). All FOC was successfully payed out.

The last flight of the day (1133 PST, figure 19) used 2.2-km length of FOC and rose to an altitude of 829 m. For this flight, the boat was held at a constant speed of 6 m/s (12 knots) from launch through FOC separation.

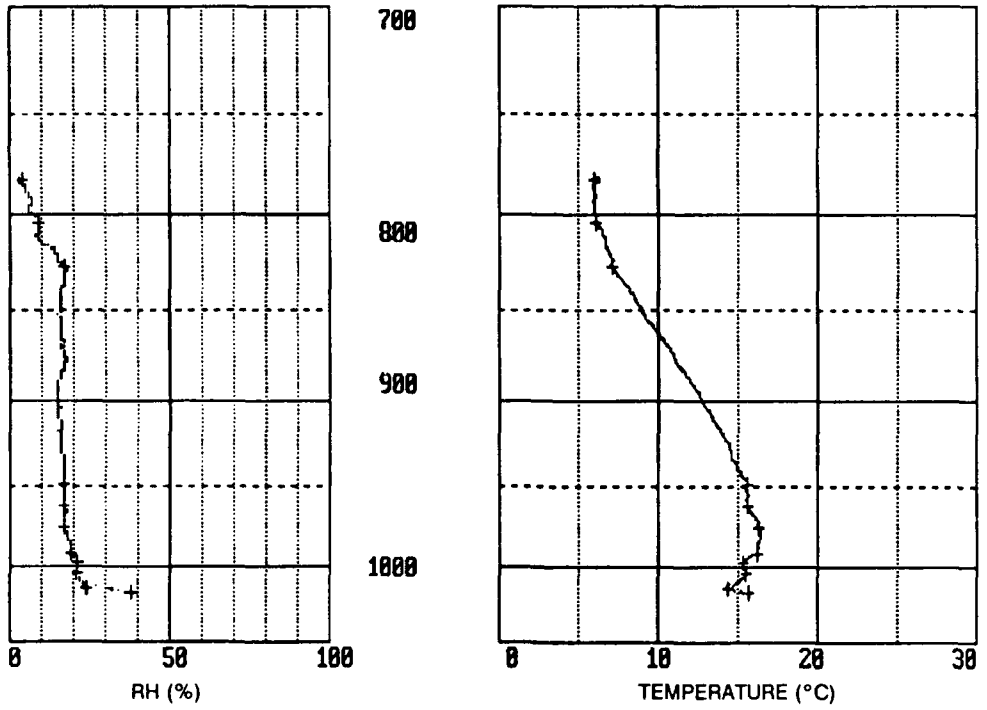

Figure 16. Pressure-altitude plot of temperature and relative humidity for the 0953 PST, 31 January 1989 flight test (at sea).

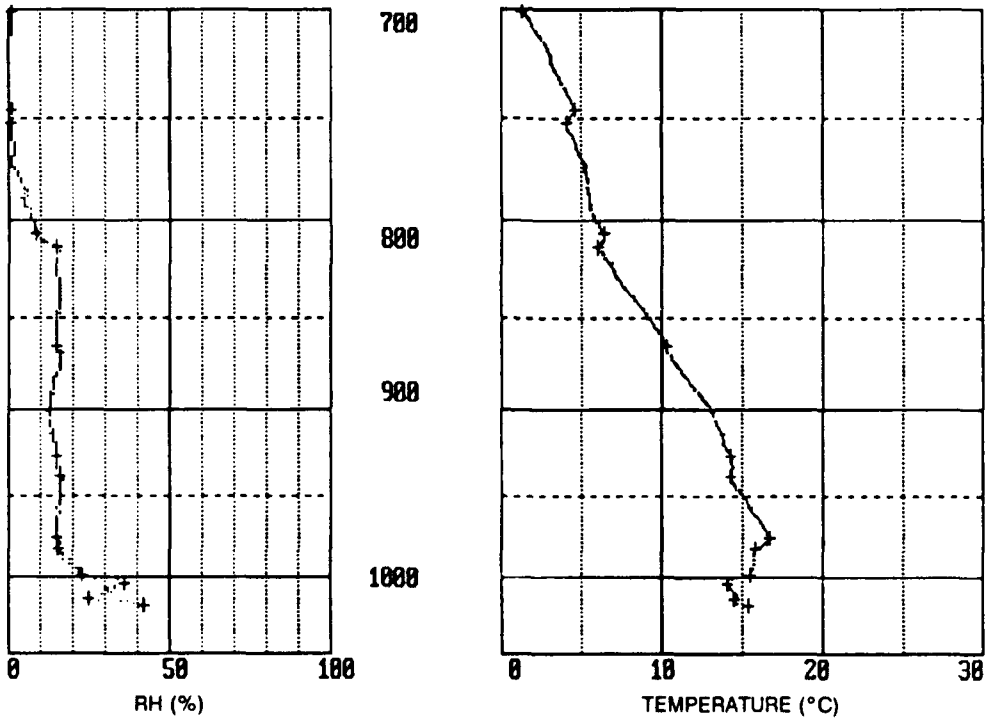

Figure 17. Pressure-altitude plot of temperature and relative humidity for the 1043 PST, 31 January 1989 flight test (at sea).

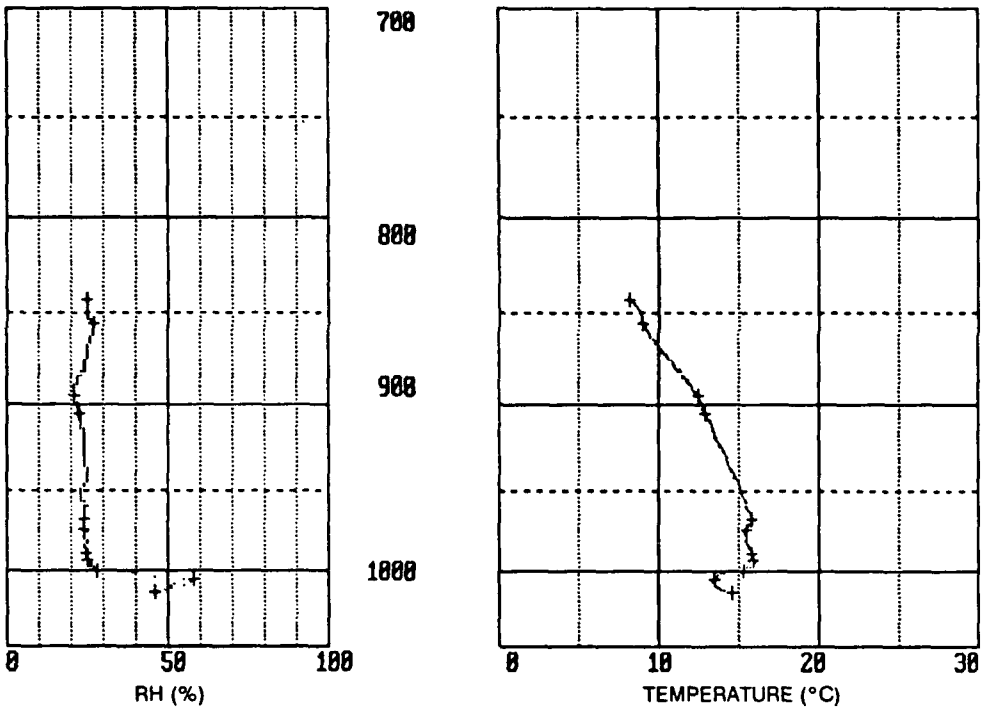

Figure 18. Pressure-altitude plot of temperature and relative humidity for the 1110 PST, 31 January 1989 flight test (at sea).

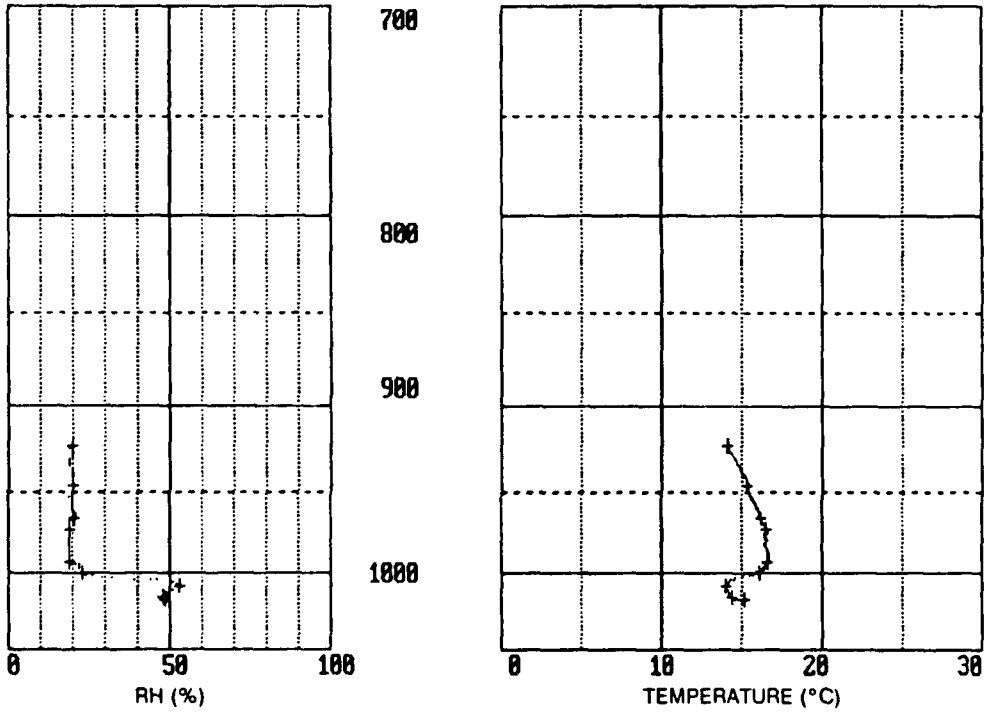

Figure 19. Pressure-altitude plot of temperature and relative humidity for the 1133 PST, 31 January 1989 flight test (at sea).

Table 8. Data from 0953 PST, 31 January 1989 flight test (at sea).

Time (s)	Press. (mbar)	Temp. (C)	RH (%)	Height (m)	M	dT (s)	dH/dT (m/s)	<dH/dT> (m/s)
6	1021.0	15.7	38	0.0	304.6			
17	1018.2	14.4	24	23.7	296.2	11	2.15	2.15
39	1008.3	15.5	21	106.4	304.3	22	3.76	3.22
53	1001.3	15.3	21	165.5	311.7	14	4.22	3.52
65	995.7	16.2	19	212.9	316.0	12	3.95	3.61
95	979.1	16.3	17	355.3	332.3	30	4.75	3.99
123	965.5	15.6	17	473.9	347.3	28	4.24	4.05
149	952.1	15.6	17	592.3	362.3	26	4.55	4.14
448	827.9	7.1	17	1758.6	513.4	299	3.90	3.98
510	805.0	6.1	9	1987.8	539.7	62	3.70	3.94
569	782.8	6.0	4	2216.6	567.3	59	3.88	3.94

Table 9. Data from 1043 PST, 31 January 1989 flight test (at sea).

Time (s)	Press. (mbar)	Temp. (C)	RH (%)	Height (m)	M	dT (s)	dH/dT (m/s)	<dH/dT> (m/s)
0	1022.5	15.4	42	0.0	307.9			
16	1018.2	14.5	25	35.5	298.8	16	2.22	2.22
40	1008.3	14.1	36	118.0	317.1	24	3.44	2.95
56	1002.7	15.5	23	165.3	313.6	16	2.96	2.95
90	986.0	15.8	16	307.4	325.5	34	4.18	3.42
106	979.1	16.7	15	366.7	332.3	16	3.71	3.46
184	941.5	14.3	16	698.1	375.5	78	4.25	3.79
211	929.7	14.3	15	804.1	388.2	27	3.93	3.81
356	867.0	10.3	15	1389.2	464.1	145	4.04	3.90
478	814.1	6.0	15	1908.0	532.5	122	4.25	3.99
495	807.3	6.4	9	1976.7	538.2	17	4.04	3.99
637	752.8	4.1	1	2546.9	610.8	142	4.02	4.00
653	746.5	4.6	1	2615.0	619.4	16	4.26	4.00
800	701.0	1.3	1	3123.9	688.8	147	3.46	3.90

Table 10. Data from 1110 PST, 31 January 1989 flight test (at sea).

Time (s)	Press. (mbar)	Temp. (C)	RH (%)	Height (m)	M	dT (s)	dH/dT (m/s)	<dH/dT> (m/s)
0	1018.2	14.6	46	0.0	309.0			
21	1009.7	13.5	58	70.8	325.2	21	3.37	3.37
39	1004.1	15.3	28	118.0	310.5	18	2.62	3.03
57	997.1	15.9	25	177.3	315.7	18	3.29	3.11
64	992.9	15.8	25	212.8	319.7	7	5.07	3.33
99	977.7	15.5	24	343.1	335.6	35	3.72	3.47
111	970.9	15.8	24	402.4	343.1	12	4.94	3.63

Table 10. Data from 1110 PST, 31 January 1989 flight test (at sea)—continued.

Time (s)	Press. (mbar)	Temp. (C)	RH (%)	Height (m)	M	dT (s)	dH/dT (m/s)	<dH/dT> (m/s)
249	907.9	12.9	23	968.4	413.5	138	4.10	3.89
268	897.8	12.5	21	1062.2	424.5	19	4.94	3.96
357	857.3	9.0	27	1446.4	477.3	89	4.32	4.05
386	844.2	8.2	25	1573.5	492.6	29	4.38	4.08

Table 11. Data from 1133 PST, 31 January 1989 flight test (at sea).

Time (s)	Press. (mbar)	Temp. (C)	RH (%)	Height (m)	M	dT (s)	dH/dT (m/s)	<dH/dT> (m/s)
2	1021.0	15.2	49	0.0	312.4			
9	1019.6	14.4	48	11.8	312.6	7	1.69	1.69
25	1012.5	14.0	53	70.8	323.1	16	3.69	3.08
44	1004.1	16.1	23	141.8	310.4	19	3.74	3.38
58	997.1	16.6	19	201.2	314.5	14	4.24	3.59
100	976.4	16.5	19	379.4	337.0	42	4.24	3.87
117	969.6	16.2	21	438.8	345.7	17	3.49	3.82
165	949.4	15.3	20	616.5	367.8	48	3.70	3.78
223	925.8	14.1	20	829.0	394.8	58	3.66	3.75

CONCLUSIONS

The feasibility of using a fiber-optic link to a modified radionsonde was successfully demonstrated. The 250-μm buffered optical fiber was strong enough to handle the stresses involved with balloon takeoff and flight using the spinning-reel wind deployment technique. The methods of receiving, filtering, and amplifying the signal proved to be adequate for the existing ground station.

The system, as a whole, functioned as expected and reliably transmitted the meteorological data to the ground. A simple, nonradiating data link from the refractionsonde instrument package to the ground station receiver is feasible for routine use.

REFERENCES

1. Hitney, H. V., J. H. Richter, R. A. Pappert, K. D.Anderson, and G.B. Baumgartner, Jr. Feb 1985. "Tropospheric Radio Propagation," *IEEE Proceedings*, vol. 73, no. 2, pp. 265-283.

2. Patterson, W. L., C. P. Hattan, H. V. Hitney, R. A. Paulus, K. D. Anderson, and G. E. Lindem. Sep 1987. "IREPS 3.0 User's Manual," NOSC TD 1151. Naval Ocean Systems Center, San Diego, CA.

3. Patterson, W. L. Oct 1988. "Effective Use of the Electromagnetic Products of TESS and IREPS," NOSC TD 1369. Naval Ocean Systems Center, San Diego, CA.

GLOSSARY

AC	alternating current
AGC	automatic gain control
C	Celsius
dB	decibel
dH	change in height
dT	change in time
ERS	electronic refractometer set
EMCON	emission control
FOC	fiber-optic cable
g	gram
IREPS	Integrated Refractive Effects Prediction System
kg	kilogram
km	kilometer
kpsi	1000 pounds per square inch
kHz	kilohertz
LED	light-emitting diode
MHz	megahertz
mbar	millibar
m	meter
M	modified refractivity
nm	nanometer
OTDR	optical time-domain reflectometer
PDT	Pacific Daylight Time
PST	Pacific Standard Time
RF	radio frequency
RH	relative humidity
s	second
TESS	Tactical Environmental Support System
TDA	tactical decision aid
UHF	ultrahigh frequency
UV	ultraviolet
V	volt
VCO	voltage-controlled oscillator
W	watt
μF	microfarad
μm	micrometer
Ω	ohm

REPORT DOCUMENTATION PAGE

Form Approved
OMB No. 0704-0188

1. AGENCY USE ONLY *(Leave blank)*	2. REPORT DATE	3. REPORT TYPE AND DATES COVERED
	April 1991	Final: Jun 1987—Jan 1991

4. TITLE AND SUBTITLE

FIBER-OPTIC REFRACTIONSONDE

5. FUNDING NUMBERS

PE: 0602435N
PROJ: RU35G80
SUBPROJ: 54-SXB3-01
ACC: DN888 715

6. AUTHOR(S)

K. D. Anderson and C. M. Young

7. PERFORMING ORGANIZATION NAME(S) AND ADDRESS(ES)

Naval Ocean Systems Center
San Diego, CA 92152-5000

8. PERFORMING ORGANIZATION REPORT NUMBER

NOSC TR 1403

9. SPONSORING/MONITORING AGENCY NAME(S) AND ADDRESS(ES)

Naval Ocean Systems Center
San Diego, CA 92152-5000

10. SPONSORING/MONITORING AGENCY REPORT NUMBER

11. SUPPLEMENTARY NOTES

12a. DISTRIBUTION/AVAILABILITY STATEMENT

Approved for public release; distribution is unlimited.

12b. DISTRIBUTION CODE

13. ABSTRACT *(Maximum 200 words)*

This report discusses tests of the prototype fiber-optic refractionsonde instrument package to see if it can send meteorological data to the ground. Both 250-μm and 500-μm buffered fiber-optic cables (FOC) were used for the land-based and at-sea tests. At first, the 500-μm FOC was thought to be desirable for use with a reel-type system because of its ruggedness and greater microbending isolation. However, tests showed the wind drag on the 500-μm buffered cable rendered it unsatisfactory. On the other hand, the 250-μm FOC was found it can withstand the stresses of balloon takeoff and flight using the spinning-reel wind deployment technique.

The refractionsionde, as a whole, performed as predicted and reliably transmitted meteorological data to the ground station.

14. SUBJECT TERMS

electronic refractometer sets (ERS)
fiber-optic cable (FOC)
radiosonde
refractionsonde
Integrated Refractive Effects Prediction (IREPS)
Tactical Environmental Support System (TESS)
tactical decision aids (TDA)

15. NUMBER OF PAGES

34

16. PRICE CODE

17. SECURITY CLASSIFICATION OF REPORT	18. SECURITY CLASSIFICATION OF THIS PAGE	19. SECURITY CLASSIFICATION OF ABSTRACT	20. LIMITATION OF ABSTRACT
UNCLASSIFIED	UNCLASSIFIED	UNCLASSIFIED	SAME AS REPORT

21a. NAME OF RESPONSIBLE INDIVIDUAL	21b. TELEPHONE *(Include Area Code)*	21c. OFFICE SYMBOL
K. D. ANDERSON	(619)553-1420	Code 543

INITIAL DISTRIBUTION

Code 0012	Patent Counsel	(1)
Code 0144	R. November	(1)
Code 50	Acting Head	(1)
Code 54	J. H. Richter	(1)
Code 543	K. D. Anderson	(25)
Code 946	S. J. Cowen	(2)
Code 952B	J. Puleo	(1)
Code 961	Archive/Stock	(6)
Code 964B	Library	(3)

Defense Technical Information Center
Alexandria, VA 22304-6145 (4)

NOSC Liaison Office
Washington, DC 20363-5100 (1)

Center for Naval Analyses
Alexandria, VA 22302-0268 (1)

Chief of Naval Operations
Washington, DC 20350-5000 (1)

Space & Naval Warfare Systems Command
Washington, DC 20363-5100 (2)

Naval Oceanography Command
Stennis Space Center, MS 39529-5000 (1)

Office of Naval Technology
Arlington, VA 22217-5000 (2)